Int. J. Electrochem. Sci., 14 **(2019)** 359 – 370, doi: 10.20964/2019.01.08

International Journal of
ELECTROCHEMICAL
SCIENCE
www.electrochemsci.org

Synthesis and Electrochemical Performance of a PEDOT:PSS@Ge Composite as the Anode Materials for Lithium-Ion Batteries

Jinfeng Liu, Jing Xu[*], *Yufang Chen, Weiwei Sun, Xiaoxiong Zhou, Jianhuang Ke*

college of Aerospace Science and Engineering, National University of Defense Technology, Chang Sha, Hu Nan, 410073, China
[*]E-mail: xujin503@163.com

Received: 18 September 2018 / *Accepted:* 16 October 2018 / *Published:* 30 November 2018

The theoretical specific capacity and volume specific capacity of Ge anode active materials can reach to 1600 $mAhg^{-1}$ and 8500 mAh/cm^3, respectively, which offers a significant advantage to high-power lithium-ion batteries used for miniaturization and weight reduction. However, the volume expansion rate of Ge is as high as 300% during cycling, resulting in poor first Coulomb efficiencies and cyclic stabilites. In this paper, a new type of organic shell (PEDOT: PSS) @ inorganic core (Ge) composite anode material for lithium ion batteries was designed and synthesized by a simple solution impregnation method . The nano-Ge anode active material was prepared by a simple liquid phase reduction method. The composition, structure and electrochemical properties of the prepared composites were analysed by field emission scanning electron microscopy (SEM), transmission electron microscopy (TEM), X-ray diffraction (XRD), energy spectrum analysis (EDS), infrared spectroscopy (FT-IR), galvanostatic charge-discharge and alternating current impedance. The results show that the conductive polymer, PEDOT:PSS, was successfully coated onto the surface of the prepared nano-Ge particles. The composite electrodes exhibits a reversible capacity of 405 $mAhg^{-1}$ after 200 cycles at 0.2C and rate capability of 800 and 700 $mAhg^{-1}$ at 2C and 4C respectively, which is much better than nanostructured Ge anodes without PEDOT:PSS coating. Meanwhile, there are higher initial discharge capacity (Up to 1400 $mAhg^{-1}$) and Coulomb efficiencies (89%, pure Ge is 81%) for PEDOT@Ge. The significantly enhanced cycle performance is attributed to the face that the PEDOT:PSS coating can effectively improve the electronic conductivity of Ge and provide buffer framework to reduce the volume change in electrochemical lithium reactions.

Keywords: PEDOT:PSS, Ge, conductive polymers, lithium-ion battery

1. INTRODUCTION

Currently, secondary batteries have achieved high conversion efficiencies for the conversion of chemical and electrical energy，and have become important energy storage devices. Among them,

lithium- ion econdary batteries have the advantages of high energy density, high power density and high working voltage[1-4]. As a new type of anode material for lithium-ion batteries, Ge has a theoretical capacity of 1600 $mAhg^{-1}$, which is more than four times the theoretical capacity of traditional graphite anode materials (372 $mAhg^{-1}$)[5]. Compared with Si anode electrodes, the electronic conductivity of Ge is 104 times that of Si, and the transmission rate of Li^+ is approximately 400 times higher than in Si anodes at room temperature, although the theoretical specific capacity of Ge is inferior (the theoretical specific capacity of Si is 4200 $mAhg^{-1}$)[6-7]. In particular, the specific volume capacity of Ge can reach 8500 mAh/cm^3, which is a significant advantage for high-power lithium-ion batteries, which are used for their small size and light weight[8-9]. Therefore, the application of Ge to the high-performance lithium ion secondary battery anode active materials is promising. However, Ge exhibits volume expansion of up to 300% during cycling, resulting in low initial Coulombic efficiency and poor cyclic stability[10-12]. The surface coating modification is an important measure to improve its electrochemical performance. Chengmao Xiao et al.[13] reported three-dimensional porous germanium nanoparticles (Ge-TPP) were prepared by acid etching of Mg_2Ge alloy, and the carbon-coated three-dimensional porous germanium nanoparticles (Ge@C TPP) were synthesized by acetylene pyrolysis and carbon deposition. The three-dimensional porous structure and carbon coating effectively alleviate the volume change during cycling, which allows the material to have good cycling stability. Dan Li et al.[14]. synthesized C/Ge/Graphene composite nanoparticles with a unique sandwich structure by microwave-assisted solvothermal reaction, which exhibited good cycle stability. Chao Zhong et al.[15] synthesized in situ Ge-GNScomposites with three-dimensional nanostructures in a simple one-step solution. Compared with the pure Ge electrode, the cycle and rate performances were significantly improved. The modification of carbon materials, including graphene, can improve the conductivity of Ge and the entire electrode. The carbon material coating, with smaller volume expansion, can effectively alleviate the volume effect of Ge anodes and improve the cycle stability[16-19]. Conductive polymers are a class of materials with good electronic conductivity and designability. They can not only effectively reduce the volume effect during cycling by forming an elastic framework around the active material nanoparticles but also bridge the isolated active nanoparticles to greatly improve the conductivity of the active material[20-21]. Poly(3,4-ethylenedioxythiophene) (PEDOT), a conductive polymer with a regular molecular chain structure and stable conductive state, is often used to modify cathode and anode materials for lithium-ion batteries[22-24]. In addition, poly(p-styrene sulfonic acid) (PSS) can be incorporated into PEDOT to form a water-soluble conductive polymer, PEDOT:PSS, with high conductivity (such as *CLEVIOS*^{TM} PH1000), which enables a polar solvent environment favouring the transmission of lithium ions[25-26]. PEDOT:PSS is a potential coating material due to its excellent chemical and mechanical stability as well as high electrical conductivity. Ko et al.[27] reported that α-Mn_2O_3/PEDOT:PSS nanowires showed significantly enhanced electrochemical performance with respect to cycle stability and rate capability after coating with PEDOT:PSS. Zhang et al. reported that PEDOT:PSS was used to coat $Li_4Ti_5O_{12}$[28], Si[29] and MoS_2 [30]. The nano-Si/PEDOT:PSS composite, prepared by chemically polymerizing PEDOT in a PSS water solution containing dispersed nanosize Si particles, showed higher initial Coulombic efficiencies and better cycling performances than the bare nano-Si composites. The MoS_2/P composite electrode delivered a reversible capacity of 712 mAh g^{-1} at a current density of 50 mA g^{-1} and retained 81% capacity after 100 cycles. The electrochemical properties

of LTO, especially the rate capability, were significantly improved by coating with a thin PEDOT:PSS layer. Bai et al.[31] reported a Ge film that was conformally coated onto CuO nanorods, and the CuO/Ge was then coated with PEDOT:PSS by spin-coating. CuO/Ge/PEDOT:PSS delivers a reversible capacity of 640 mAh g^{-1} after 1000 cycles at a current density of 2 A g^{-1}. The excellent electrochemical performance can be ascribed to the PEDOT:PSS coating.

In this paper, the conductive polymer PEDOT:PSS was used to coat the surface of a Ge anode active material by a facile and convenient approach, and the PEDOT:PSS@Ge composite anode material was prepared by the impregnation-coating method for the first time. The preparation process is shown in Fig. 1. Coating PEDOT:PSS on the surface of Ge anode active materials can improve its electronic conductivity and the transmission rate of Li^+, reduce the irreversible change in volume during cycling, and improve the electrochemical performance of the Ge negative electrode material.

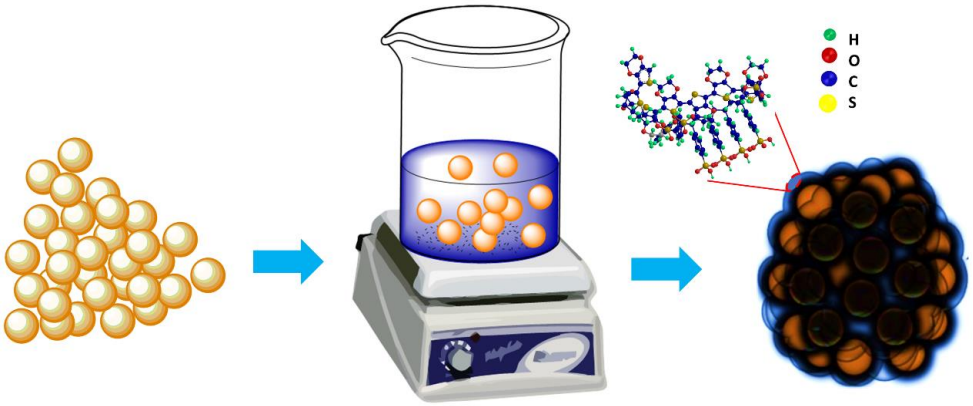

Figure 1. Schematic illustration of the fabrication of the PEDOT:PSS@Ge

2. EXPERIMENT

2.1 Preparation of PEDOT:PSS@Ge

GeO_2 (0.26 g) was dissolved in a 0.5 mol/L NaOH solution of 15 ml. When it was completely dissolved, and the solution was transparent, 0.01 g PVP was added as a dispersing agent. A 5% HCl solution was added dropwise into the above solution to adjust the pH to neutral (solution A). $NaBH_4$ (0.47 g) was dissolved in deionized water (0-4 °C), quickly added to solution A, and the reaction was stirred rapidly for 3-5 h to obtain a dark brown suspension. After centrifugation, the precipitate was washed repeatedly until the washing solution was neutral and then dried in a vacuum drying box to obtain Ge nanoparticles.

The 1 g of Ge nanoparticles prepared by the above method was dispersed in deionized water and ultrasonicated for 20 min so that they were uniformly dispersed. Then, 3 ml of PEDOT:PSS (*CLEVIOS*^{TM} PH1000, solid content 1%) was added to the above solution, which was then stirred and volatilized at 60 °C. After the solvent was evaporated, it was placed into a vacuum oven at 80 °C for 24 h after grinding to obtain the PEDOT:PSS@Ge composite material.

2.2 Materials Characterization

The surface morphology and energy spectrum of the samples were observed with a Japanese HITACHIS 4800 field emission scanning electron microscope (SEM) and a US FEIT F20 field emission transmission electron microscope (TEM). The crystal structures of the Ge and PEDOT:PSS@Ge samples were studied by X-ray diffraction (Bruk-D8X) equipped with Cu Kα radiation (= 0.15406 nm). The functional groups of the samples were detected with an Alpha-P infrared spectrometer (FTIR).

2.3 Electrochemical Measurements

N-Methylpyrrolidone (NMP) was used as the solvent, and the PEDOT:PSS@Ge composite material, conductive carbon black and PVDF were ground into an electrode slurry at a mass ratio of 8:1:1 and then uniformly coated onto the surface of copper foil and dried under vacuum at 80 ° C. Then, it was cut into 15 mm electrode sheets, and the button cell was assembled using Celgard 2400 polypropylene multilayer membrane as the separator, and 1.0 mol/L $LiPF_6$ (EC: DMC=1:1) as the electrolyte. The constant current charge and discharge test was carried out using a Wuhan LAND CT2001A instrument with a voltage range of 1.5-0 V, and charge and discharge rates of 0.2 C (1 C=1600 $mAhg^{-1}$); the AC impedance (EIS) was measured by with a VersaSTAT MC electrochemical workstation. The frequency range was 0.01-106 HZ, and the voltage range was 1.5-0 V.

3. RESULTS AND DISCUSSION

The SEM and TEM images of nano-Ge and PEDOT:PSS@Ge and the energy spectra for the distribution of each element are shown in Fig. 2. As seen from Fig. 2 (a), the particle size of the prepared nano-Ge is in the range of 10-100 nm, which is mainly due to the large surface energy of the nano-Ge resulting in agglomeration during the preparation process. At the same time, it can be seen that the surface of the nano-Ge particles is smooth. Fig. 2(b) is an SEM image of the conductive PEDOT:PSS @Ge particles. Combined with the TEM image (Fig. 2d), it shows that the nano-Ge particles are coated by the conductive polymer. PEDOT:PSS and Ge formed a micro-nano hierarchical structure with an organic shell/inorganic core. The distribution of S can be found to be even from the energy spectra in Fig. 2(d-g), indicating the PEDOT:PSS uniformly exists on the surface of nano-Ge anode. The micro-nano hierarchical structure provides an organic PEDOT:PSS framework to the nano-Ge anode active material, which can bind the nano-Ge particles, reduce the volume effect during electrochemical cycling, and simultaneously improve the electronic conductivity of the Ge anode.

The phase and purity of nano-Ge and PEDOT:PSS@Ge were identified by X-ray diffraction (XRD), as shown in Fig. 3 (a). The diffraction peaks located at 2θ=27°,45°,54°,66°,73° and 84° in the crystal structure of the nano-Ge materials correspond to the crystal planes of (111), (220), (311), (400), (331) and (422), respectively. There are no other heterophase diffraction peaks, indicating that the prepared nano-Ge active electrode materials have good crystallinity[32-34]. Comparing the XRD spectra of PEDOT:PSS@Ge, it is found that the coating of conductive polymer does not change the

diffraction characteristics of Ge, such as the position and width of the diffraction peak, indicating that the modification of PEDOT:PSS has no significant effect on the crystal structure of Ge. FTIR spectroscopy was used to characterize the formation of the PEDOT:PSS@Ge composite. Fig. 3(b) presents the FTIR spectra of the PEDOT:PSS@Ge composite, along with those of PEDOT and nano-Ge particles for comparison. The absorption peak is very obvious at 840 cm^{-1}, corresponding to the characteristic peak of nano-Ge. The –C–S– bond at 980 cm^{-1}, the stretching vibration of the –C–O–C– bond at 1090 cm^{-1}, and the asymmetric C=C in the thiophene loop stretching at 1522 cm^{-1} were clearly observed in the spectrum of PEDOT:PSS and PEDOT:PSS@Ge. Furthermore, the characteristic peaks at 1170, 1129 and 690 cm^{-1} correspond to S-O, S-phenyl and C-S-C stretching vibrations, respectively[29, 35].The SEM,TEM and FT-IR results demonstrate that the conductive polymer layer (PEDOT:PSS) well covers on the surface of nano-Ge anode active materials[25, 29]. Here, we can speculate that this coating layer can suppress the undesired volume change, benefit the diffusion of electron and Li-ion through the interface layer during cycling.

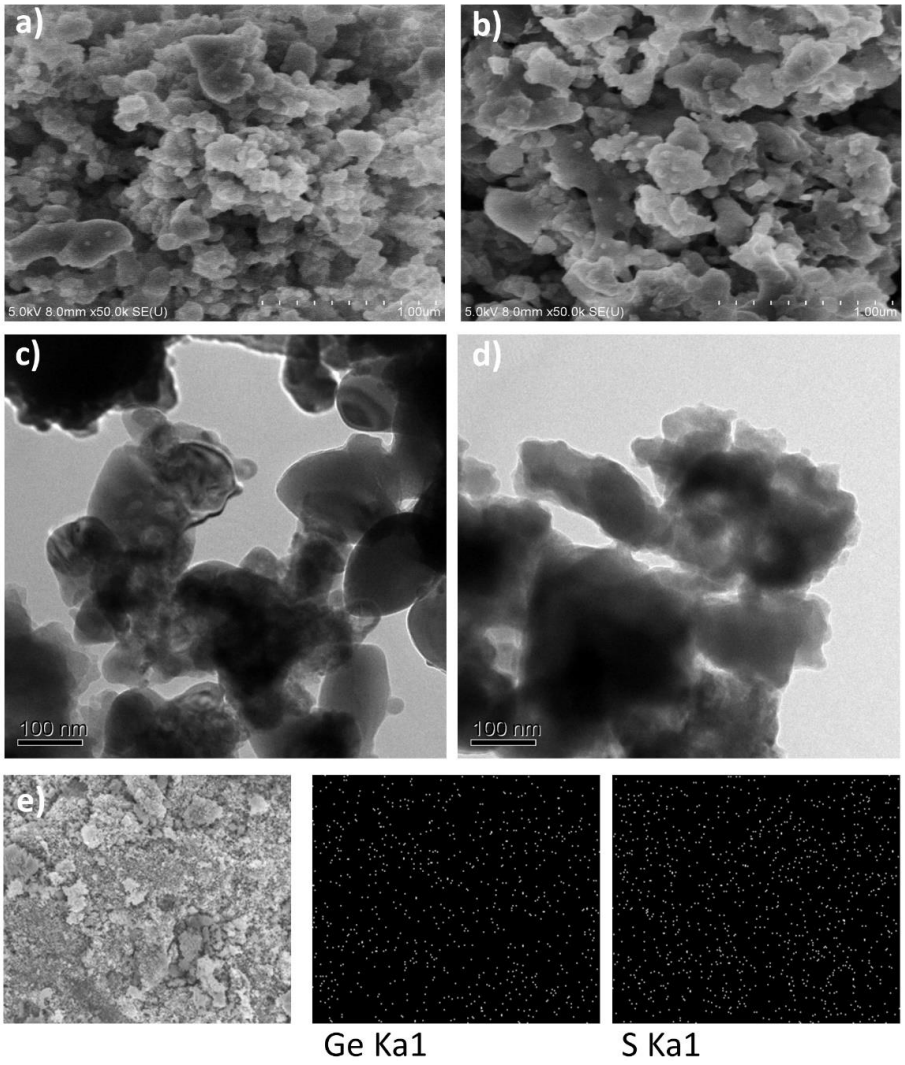

Figure 2. SEM and TEM images of bare Ge (a, c), PEDOT:PSS@Ge (b, d), and SEM (e) of PEDOT:PSS@Ge and the related EDS mapping images

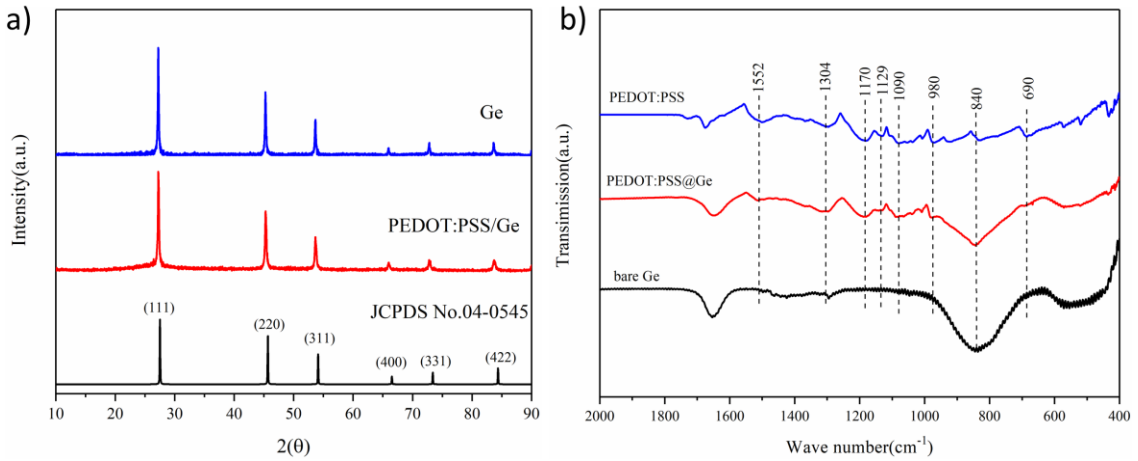

Figure 3. XRD pattern (a), and FTIR spectra (b)of Ge and PEDOT:PSS@Ge

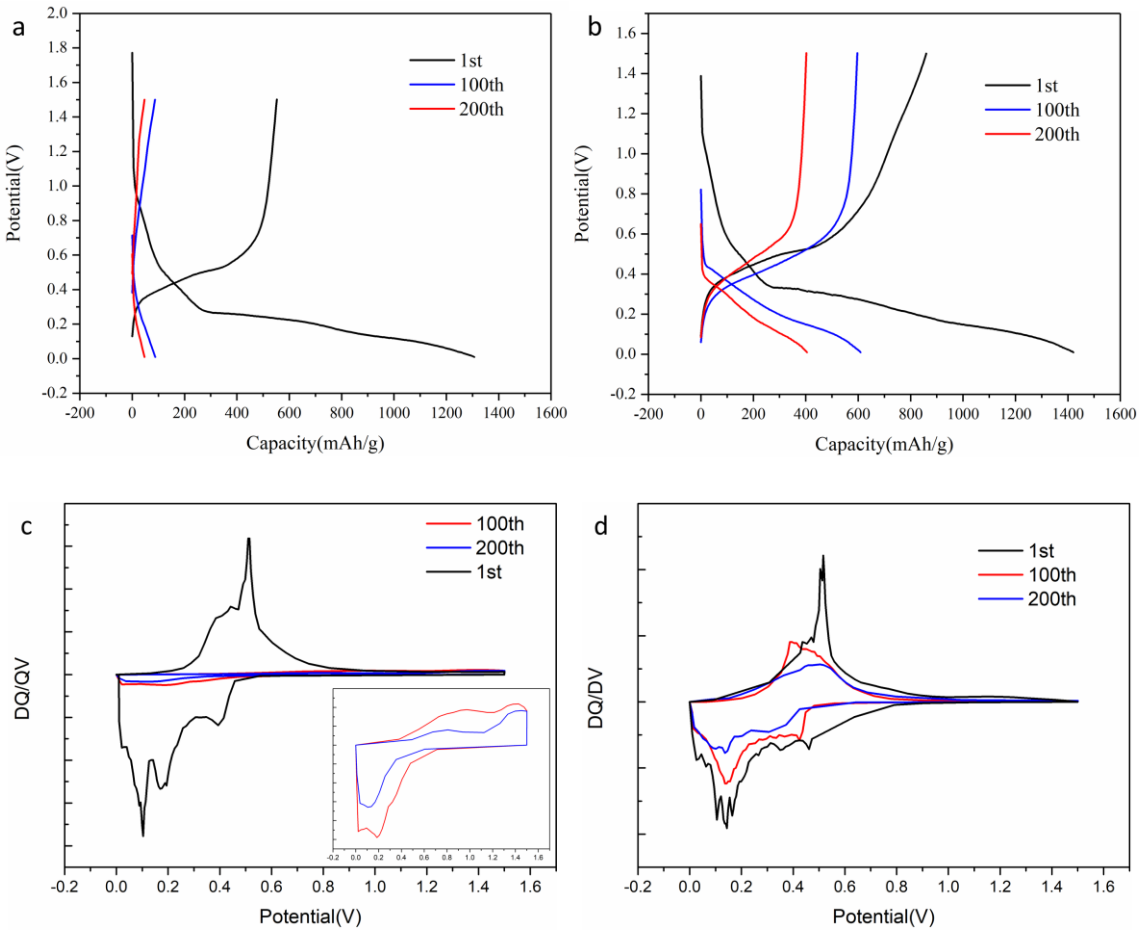

Figure 4. 1st, 100th and 200th charge–discharge and DQ/DV-V curves of Ge (a, c) and PEDOT:PSS@Ge (b, d) at 0.2 C and room temperature (25 ℃).

The charge-discharge curves and corresponding DQ/DV-V curves of nano-Ge and PEDOT:PSS@Ge anode materials for the 1st, 100th and 200th times are shown in Fig. 4. The initial discharge capacity and Coulombic efficiency of PEDOT:PSS@Ge were 1450 $mAhg^{-1}$ and 90.5%, respectively. In contrast, the first discharge capacity of the nano-Ge is 1300 $mAhg^{-1}$, and the Coulombic efficiency is 9.3%, which is lower than that of the PEDOT:PSS@Ge active anode material. From the

DQ/DV-V curves, it can be seen that the redox peak of the pure Ge anode material shifted by 0.32 V compared with the 1st and 100th cycles, and the shift increased to 0.4 V after 200 cycles. However, the redox peak position of the Ge modified by PEDOT:PSS only shifted by 0.08 V after 100 cycles, while after 200 cycles, the shift was only 0.1 V. The difference between the characteristic peaks of PEDOT:PSS@Ge, after the extraction-insertion process of lithium ions, is obviously smaller than that of the pristine nano-Ge anode. This shows that the introduction of the conductive polymer in PEDOT:PSS@Ge makes the nano-Ge anode active material have a smaller polarization impedance. The 100th discharge capacity of pure nano-Ge and PEDOT:PSS@Ge are 90.1 $mAhg^{-1}$ and 617 $mAhg^{-1}$, respectively. Compared with the first discharge, the capacity of bare Ge dropped by 93%, while that of PEDOT:PSS@Ge dropped by 57.4%. Similarly, the discharge capacity of pure Ge after 200 times is only 47 $mAhg^{-1}$, while that of PEDOT:PSS@Ge is still 405 $mAhg^{-1}$ thus, the capacity retention rate is 24.4% higher than that of pure Ge. The slower voltage fading and higher coulombic efficiency and discharge capacity retention of the coated electrode can be ascribed to the protective effect of PEODT:PSS coating layer, which not only enhances the structure stability of anode, but also reduces the polarization to form a stable surface state.

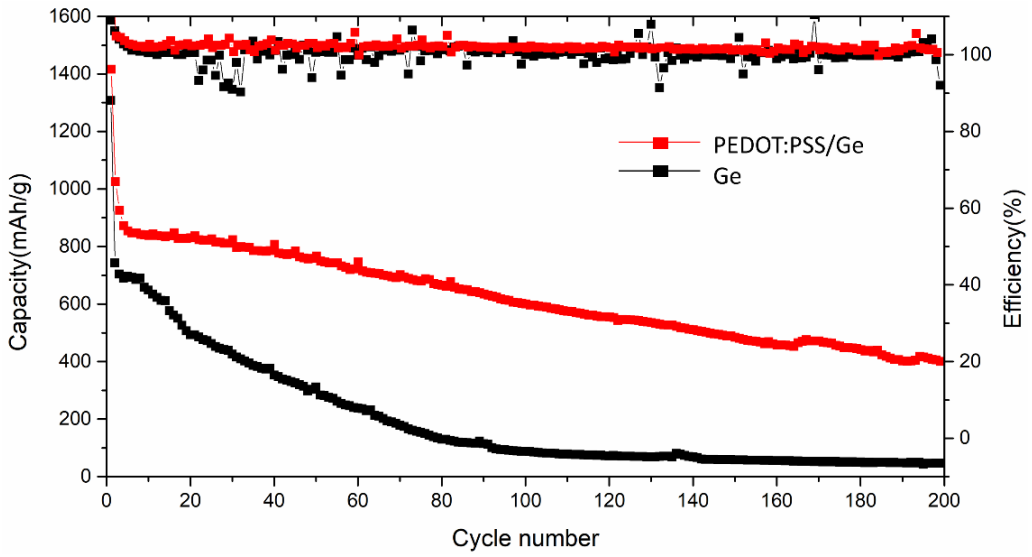

Figure 5. Cycle-capacity curve and charge-discharge efficiency of Ge and PEDOT:PSS@Ge composite anode active materials at 0.2C

The cycling performance of nano-Ge and PEDOT:PSS@Ge at 0.2 C is displayed in Fig. 5. To further understand the modification of PEDOT:PSS to anode materials, synthesis method and electrochemical performance of the different anode active materials coated by PEDOT:PSS are shown in Table.1. As mentioned earlier, PEDOT:PSS has excellent chemical and mechanical stability as well as high electrical conductivity, it Can effectively improve the electrochemical properties of the anode material such as Mn_2O_3[27], $Li_4Ti_5O_{12}$[28], Si[29], , MoS_2[30] , and CuO/Ge[31] and so on. However, the preparation process of spin-coating CuO/Ge with PEDOT:PSS is complicated and is not suitable for commercial applications. The PEDOT:PSS@Ge electrode synthesized by a simple solution impregnation method showed improved cycling performance compared with the nano-Ge electrode

without polymer coating. It delivers a high first discharge capacity of 1450mAh/g, and after 200 cycles at 0.2C, its discharge capacity is still 405mAh/g. At the same time, according to the comparison of the charge-discharge efficiency in the long cycle, we found that the Coulombic efficiency of bare Ge is lower, and its distribution is more disperse. The greater retention can be attributed only to volume change that results in the material structure being less stable during the cycle. In contrast, surprisingly, PEDOT:PSS@Ge has a higher initial discharge capacity, and the Coulombic efficiency during cycling is more stable, indicating that PEDOT:PSS@Ge has better cycle stability.

Table 1. Synthesis method and electrochemical performance of the different anode active materials coated by PEDOT:PSS

Anode Materials	Synthesis method	Optimally coated samples	Electrochemical properties including inital specific capacity, capacity retention(cycles, rate)	Ref.
α-Mn_2O_3	Sonicate	α-Mn_2O_3/PEDOT:PSS	1450(200,100mA g^{-1})	[27]
$Li_4Ti_5O_{12}$	Rota-evaporation	$Li_4Ti_5O_{12}$/PEDOT:PSS	172.9, 97.8%(100,0.5C)	[28]
Si	*In-situ* polymerization	Si/PEDOT:PSS	1096,60.58%(20,100 mA g^{-1})	[29]
MoS_2	dip-coating	MoS_2/ PEDOT:PSS	712 ,81%(100,50 mA g^{-1})	[30]
Ge	spin-coating	CuO/Ge/PEDOT:PSS	980,90%(1000, 2 A g^{-1})	[31]
Ge	solution impregnation method	PEDOT:PSS@Ge	1450,57.4%(200,320mA g^{-1})	This paper

The discharge capacity of Ge and the composite PEDOT:PSS@Ge at different discharge rates (0.1, 0.2, 0.5, 1, 2, 4 C) is shown in Fig. 6. It is shown that the composite exhibits excellent rate performance at different current densities. Even at high current densities of 2 and 4 C, the composite delivers specific capacities of 800 and 700 mAh g^{-1}, respectively. Moreover, the specific capacity returned to 900 mAh g^{-1} when the discharge rate returned to 0.1 C. In contrast, the discharge specific capacity of the pure Ge anode material continues to decrease as the charge-discharge rate increases. When the discharge rate increases from 0.2 to 2 C, the discharge specific capacity of the Ge anode material continues to decrease from 780 $mAhg^{-1}$ to 0. Furthermore, the discharge specific capacity of bare Ge can only recover 300 $mAhg^{-1}$ as the current density is returned to 0.1 C. PEDOT:PSS coating modification is beneficial to the improvement of electrode material rate performance, which is likely ascribed to the promotion of electronic conductivity and structural stability of the Ge anode material.

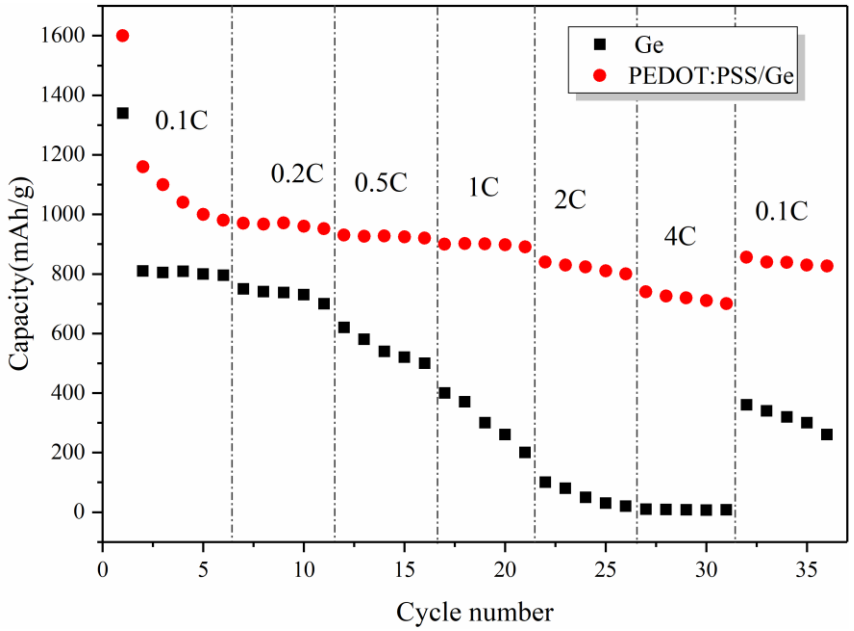

Figure 6. the rate performance of Ge and PEDOT:PSS@Ge

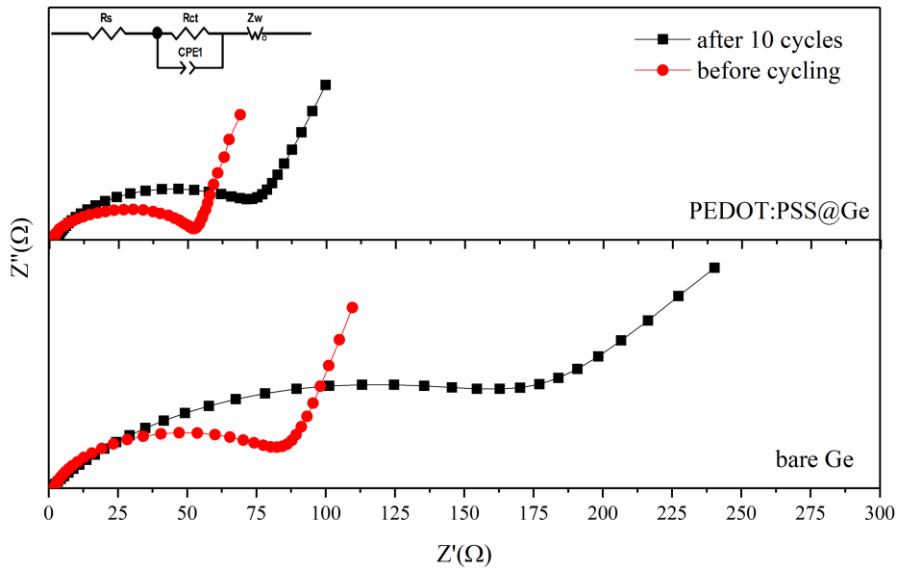

Figure 7. Nyquist plots of the bare Ge and PEDOT@Ge before cycling and after 10 cycles

The electrochemical impedance spectrum (EIS) provides further information on the kinetics of the electrochemical reactions at the electrodes. To better understand its electrochemical performance, the impedance of Ge and PEDOT:PSS@Ge was measured before and after 10 cycles. The Nyquist plots are shown in Fig. 7. According to the impedance curves before and after cycling, there is a compressed semicircle from the high to intermediate frequency range, which can be attributed to the interface layer impedance and electronic charge-transfer impedance (Rct). An inclined line in the low frequency region, which can be associated with the Warburg impedance, is related to the impedance of the lithium ion transmission (Zw)[29, 36-37]. The charge-transfer impedance of PEDOT:PSS@Ge

is 54 Ω before cycling, which is significantly lower than that of pure nano-Ge, which is 85 Ω. This further indicates that the surface modification of the conductive polymer can improve the electronic conductivity of Ge and reduce its interface and charge transfer impedances. Comparing the evolution of the impedance after 10 cycles, the Rct increased from 85 Ω to 174 Ω for bare nano-Ge anode material, an increase of 89 Ω. Surprisingly, the change of impedance (from 54 Ω to 74 Ω) was less for nano-Ge modified by the conductive polymer after 10 cycles. This shows that the structure of the organic PEDOT:PSS shell/nano-Ge core provides a conductive bridge between electrolyte and Ge anode, which can enhance the structure stability of electrode, and facilitate the fast diffusion of the electrons through the interface layer[38]. We believe that the PEDOT:PSS coating layer can improve the electrochemical performance of the nano-Ge anode material.

4. CONCLUSIONS

In this paper, a conductive polymer-coated Ge anode material was prepared by a simple and feasible solution impregnation method for the first time. SEM, TEM, XRD and FT-IR measurements showed that nanosized Ge particles were coated by PEDOT:PSS and formed a micro-nano hierarchical structure with an organic shell/inorganic core. The conductive polymer, PEDOT:PSS, significantly reduces the interfacial impedance of the Ge electrode and the lithium ion de-embedding polarization impedance, which decreased from 0.4 V for bare Ge to 0.1 V after 200 cycles. At the same time, there are higher initial discharge capacities (up to 1400 mAh/g) and Coulombic efficiencies (89%, pure Ge is 81%) for PEDOT:PSS@Ge. Furthermore, the electrode made of PEDOT:PSS@Ge delivered a more stable output capacity of 405 $mAhg^{-1}$, with a capacity retention of 28% after 200 cycles, compared with bare Ge with 47 $mAhg^{-1}$ and 3.6%, respectively. This was mainly ascribed to the binding effect of the organic shell composed of the conducting polymers. Meanwhile, the PEDOT:PSS coated material exhibited excellent rate performances of 800 mAh g^{-1} and 700 mAh g^{-1} at 2 and 4 C, respectively, due to the high electrical conductivity. However, the discharge capacity has been reduced to 0 mAh g^{-1} at a rate of 2 C. The results show that the organic shell /inorganic core structure formed by PEDOT:PSS@Ge can make full use of the excellent conductive properties of the conductive polymers and the binding effect of the polymer shell to reduce the volume effect of nano-Ge and improve the cyclic stability and rate performance of Ge anode materials.

ACKNOWLEDGEMENTS
The authors acknowledge the financial support from the National Natural Science Foundation of China (grant No. 21875282), Hunan Provincial Natural Science Foundation (grant No. 2018JJ3595), the National Postdoctoral Program for Innovative Talents (BX201700103) and China Postdoctoral Science Foundation funded project (2018M633664)

References

1. G. Xu, C. Pang, B. Chen, J. Ma, X. Wang, J. Chai, Q. Wang, W. An, X. Zhou, G. Cui, L. Chen, *Advanced Energy Materials*, 8 (2018) 1870038.

2. K. Liu, Y. Liu, D. Lin, A. Pei, Y. Cui, *Science Advances*, 4 (2018) eaas9820
3. S. Cosentino, G. Torrisi, R. Raciti, M. Zimbone, I. Crupi, S. Mirabella, A. Terrasi, *RSC Adv.*, 6 (2016) 38454.
4. W. Wei, A. Tian, F. Jia, K. Wang, P. Qu, M. Xu, *RSC Adv.*, 6 (2016) 87440
5. X. Xiao, X. Liu, H. Zhao, D. Chen, F. Liu, J. Xiang, Z. Hu, Y. Li, *Advanced Materials*, 24 (2012) 5762.
6. G. Cui, L. Gu, L. Zhi, N. Kaskhedikar, P. A. Van Aken, K. Müllen, J. Maier, *Advanced Materials*, 20 (2010) 3079.
7. M. H. Park, K. Kim, J. Kim, J. Cho, *Advanced Materials*, 22 (2010) 415.
8. D. J. Xue, S. Xin, Y. Yan, K. C. Jiang, Y. X. Yin, Y. G. Guo, L. J. Wan, *Journal of the American Chemical Society*, 134 (2012) 2512.
9. M. H. Seo, M. Park, K. T. Lee, K. Kim, J. Kim, J. Cho, *Energy & Environmental Science*, 4 (2011) 425.
10. D. Liu, Z. J. Liu, X. Li, W. Xie, Q. Wang, Q. Liu, Y. Fu, D. He, *Small*, 13 (2017) UNSP 170200.
11. D. T. Ngo, H. T. T. Le, C. Kim, J.-Y. Lee, J. G. Fisher, I.-D. Kim, C.-J. Park, *Energy & Environmental Science*, 8 (2015) 3577.
12. H. Guo, B. Ruan, L. Liu, L. Zhang, Z. Tao, S. Chou, J. Wang, H. Liu, *Small*, 13 (2017) 1700920
13. C. Xiao, N. Du, Y. Chen, J. Yu, W. Zhao, D. Yang, *RSC Adv.*, 5 (2015) 63056.
14. D. Li, K. Seng, D. Shi, Z. Chen, H. Liu, Z. Guo, *Journal of Materials Chemistry A*, 1 (2013) 14115.
15. C. Zhong, J. Z. Wang, X. W. Gao, D. Wexler, H. K. Liu, *Journal of Materials Chemistry A*, 1 (2013) 10798.
16. Y. Chen, C. Yan, O. G. Schmidt, *Advanced Energy Materials*, 3 (2013) 1269.
17. H. Jia, C. Stock, R. Kloepsch, X. He, J. P. Badillo, O. Fromm, B. Vortmann, M. Winter, T. Placke, *Acs Applied Materials & Interfaces*, 7 (2015) 1508.
18. H. Jia, R. Kloepsch, X. He, J. P. Badillo, M. Winter, T. Placke, *Journal of Materials Chemistry A*, 2 (2014) 17545.
19. D. T. Ngo, R. S. Kalubarme, H. T. Le, C. N. Park, C. J. Park, *Nanoscale*, 7 (2015) 2552.
20. S. Zhang, R. Hu, *Materials Letters*, 176 (2016) 131.
21. S. A. Abbas, M. A. Ibrahem, L.-H. Hu, C.-N. Lin, J. Fang, K. M. Boopathi, P.-C. Wang, L.-J. Li, C.-W. Chu, *J. Mater. Chem. A*, 4 (2016) 9661.
22. H. Yan, G. Zhang, Y. Li, *Applied Surface Science*, 393 (2017) 30.
23. J. Lee, W. Choi, *Journal of the Electrochemical Society*, 162 (2015) A743.
24. X. Fan, C. Luo, J. Lamb, Y. Zhu, K. Xu, C. Wang, *Nano Letters*, 15 (2015) 7650.
25. J. M. Kim, H. S. Park, J. H. Park, T. H. Kim, H. K. Song, S. Y. Lee, *ACS Appl Mater Interfaces*, 6 (2014) 12789.
26. F. Wu, J. Liu, L. Li, X. Zhang, R. Luo, Y. Ye, R. Chen, *ACS Appl Mater Interfaces*, 8 (2016) 23095.
27. I.-H. Ko, S.-J. Kim, J. Lim, S.-H. Yu, J. Ahn, J.-K. Lee, Y.-E. Sung, *Electrochimica Acta*, 187 (2016) 340.
28. Y. Liu, D. Tang, H. Zhong, Q. Zhang, J. Yang, L. Zhang, *RSC Adv.*, 6 (2016) 95512.
29. L. Yue, S. Wang, X. Zhao, L. Zhang, *J. Mater. Chem.*, 22 (2012) 1094.
30. X. Zhao, Y. Mai, H. Luo, D. Tang, B. Lee, C. Huang, L. Zhang, *Applied Surface Science*, 288 (2014) 736.
31. S. Bai, Y. Ma, X. Jiang, Q. Li, Z. Yang, Q. Liu, D. He, *Surfaces and Interfaces*, 8 (2017) 214.
32. D. Shao, H. Zhong, L. Zhang, *Chemelectrochem*, 1 (2015) 1679.
33. B. Wang, Z. Wen, J. Jin, X. Hong, S. Zhang, K. Rui, *Journal of Power Sources*, 342 (2017) 521.
34. X. Zhong, J. Wang, W. Li, X. Liu, Z. Yang, L. Gu, Y. Yu*, *RSC Adv.*, 4 (2014) 58184.
35. G. Hasegawa, *Journal of Materials Chemistry*, 21 (2011) 2060.
36. Z. Liu, Y. Luo, M. Zhou, W. Wang, N. Gan, S. Okada, J. I. Yamaki, *Electrochemistry*, 83 (2016) 1067.

37. J. S. Gnanaraj, M. D. Levi, E. Levi, G. Salitra, D. Aurbach, J. E. Fischer, A. Clayeb, *Journal of the Electrochemical Society*, 148 (2001) A525
38. J.-Z. Kong, L.-P. Xu, C.-L. Wang, Y.-X. Jiang, Y.-Q. Cao, F. Zhou, *Journal of Alloys and Compounds*, 719 (2017) 401.